Title

The Shr receptor from Streptococcus pyogenes uses a cap and release mechanism to acquire heme—iron from human hemoglobin

Journal

Proceedings of the National Academy of Sciences of the United States of America, 120(5)

ISSN

0027-8424

Authors

Macdonald, Ramsay

Mahoney, Brendan J

Soule, Jess

et al.

Publication Date

2023-01-31

DOI

10.1073/pnas.2211939120

Peer reviewed

PNAS RESEARCH ARTICLE | BIOCHEMISTRY OPEN ACCESS

The Shr receptor from *Streptococcus pyogenes* uses a cap and release mechanism to acquire heme–iron from human hemoglobin

Ramsay Macdonald[a,1], Brendan J. Mahoney[a,b,1], Jess Soule[a], Andrew K. Goring[a], Jordan Ford[a], Joseph A. Loo[a,b,c], Duilio Cascio[b], and Robert T. Clubb[a,b,c,2]

Edited by Ralph Isberg, Tufts University School of Medicine, Boston, MA; received July 22, 2022; accepted December 19, 2022

Streptococcus pyogenes **(group A *Streptococcus*) is a clinically important microbial pathogen that requires iron in order to proliferate. During infections, *S. pyogenes* uses the surface displayed Shr receptor to capture human hemoglobin (Hb) and acquires its iron-laden heme molecules. Through a poorly understood mechanism, Shr engages Hb via two structurally unique N-terminal Hb-interacting domains (HID1 and HID2) which facilitate heme transfer to proximal NEAr Transporter (NEAT) domains. Based on the results of X-ray crystallography, small angle X-ray scattering, NMR spectroscopy, native mass spectrometry, and heme transfer experiments, we propose that Shr utilizes a "cap and release" mechanism to gather heme from Hb. In the mechanism, Shr uses the HID1 and HID2 modules to preferentially recognize only heme-loaded forms of Hb by contacting the edges of its protoporphyrin rings. Heme transfer is enabled by significant receptor dynamics within the Shr–Hb complex which function to transiently uncap HID1 from the heme bound to Hb's β subunit, enabling the gated release of its relatively weakly bound heme molecule and subsequent capture by Shr's NEAT domains. These dynamics may maximize the efficiency of heme scavenging by *S. pyogenes*, enabling it to preferentially recognize and remove heme from only heme-loaded forms of Hb that contain iron.**

group A *Streptococcus* | heme capture | hemoglobin | X-ray crystallography | NMR

Significance

Bacterial infections are a major cause of death in the United States. *Streptococcus pyogenes* and other clinically important pathogens need iron to grow, which they can obtain from human hemoglobin located within red blood cells. We have learned how *S. pyogenes* uses the Shr receptor to capture hemoglobin and its iron-containing heme molecules. We propose that this process occurs via a "cap and release" mechanism in which Shr forms a dynamic complex with hemoglobin that enables the gated release of its most labile heme molecule. The mechanism reveals how many streptococci and clostridia bacterial species acquire heme and could facilitate the development of new therapeutics that starve bacteria of iron.

To successfully mount infections bacterial pathogens must overcome host nutritional immunity mechanisms that limit access to iron, an essential metal nutrient required for microbial survival because it functions as a cofactor in enzymes that mediate cellular metabolism. Human hemoglobin (Hb) contains ~75 to 80% of the body's total iron in the form of heme (iron–protoporphyrin IX) and is thus a prime nutrient source for invading microbes (1–9). Bacteria gain access to Hb's iron-laden heme molecules when erythrocytes are ruptured by bacterial cytotoxins or when they spontaneously lyse. In gram-positive monoderm bacteria, extracellular Hb is captured by surface-displayed microbial receptors. Hb's heme molecules are then released and transferred via microbial heme-binding chaperones across the expanse of the peptidoglycan to the membrane, where they are imported into the cell and degraded to release iron. The acquisition mechanisms that many pathogens use to bind to Hb and remove its tightly bound heme molecules are not well understood. *Streptococcus pyogenes* (group A *Streptococcus*) colonizes the skin and mucosal surfaces in humans and is estimated to cause more than 500,000 deaths annually (10–12). It causes a range of illnesses, ranging from acute pharyngitis to life-threatening diseases such as scarlet fever, bacteremia, pneumonia, necrotizing fasciitis, myonecrosis, and streptococcal toxic shock syndrome (13, 14). *S. pyogenes* employs the streptococcal hemoprotein receptor (Shr) to capture Hb and acquire its heme molecules, and it is an important virulence factor that when genetically deleted reduces the ability of the pathogen to grow in human blood and to cause infections in murine and zebrafish models (15–17). Strategies that interfere with the ability of *S. pyogenes* and other pathogenic bacteria to harvest heme from Hb could be useful in treating infections, as they would effectively starve pathogens of iron.

The *S. pyogenes* Shr protein is a structurally unique multidomain Hb receptor that is also found in other streptococci and clostridia species (e.g., *Clostridium novyi*, *Streptococcus iniae*, *Streptococcus equi*, and *Streptococcus dysgalactiae*) (Fig. 1*A*). Its N-terminal region (NTR, residues 26 to 364) binds to Hb using two Hb interacting domains (HIDs), called HID1 and HID2 (formally known as DUF1533 domains) (18, 19). The HIDs are structurally novel binding modules and are joined via a structured linker domain (L) to a C-terminal region (CTR, residues 365 to 1,275) which contains two heme-binding NEAr iron Transporter domains (NEAT domains N1 and N2) that are separated by a series of

Author contributions: R.M., B.J.M., J.S., and R.T.C. designed research; R.M., B.J.M., J.S., A.K.G., and J.F. performed research; A.K.G. contributed new reagents/analytic tools; R.M., B.J.M., J.S., A.K.G., J.F., and D.C. analyzed data; and R.M., B.J.M., J.S., A.K.G., J.A.L., and R.T.C. wrote the paper.

The authors declare no competing interest.

This article is a PNAS Direct Submission.

[1]R.M. and B.J.M. contributed equally to this work.

[2]To whom correspondence may be addressed. Email: rclubb@mbi.ucla.edu.

This article contains supporting information online at https://www.pnas.org/lookup/suppl/doi:10.1073/pnas.2211939120/-/DCSupplemental.

Published January 24, 2023.

leucine-rich repeats (LRR). The NTR and N1 domain within Shr (called NTR-N1) preferentially bind to holo-Hb and remove its heme (18). In vitro, heme bound by the N1 domain is then readily transferred to either the C-terminal N2 domain, or to Shp, a cell wall-associated protein that relays heme to the membrane-associated HtsABC/SiaABC transporter that pumps heme into the cytoplasm (20–22). The N2 domain in Shr may act as a storage unit, since it binds to heme with much higher affinity than N1 and does not directly transfer heme to Shp (23). Shr also interacts via its N2 domain with the human extracellular matrix (ECM) proteins fibronectin and laminin (15, 16, 18), and its exposure on the cell surface may make it a useful epitope in *S. pyogenes* vaccines (24, 25). However, it remains poorly understood how Shr acquires heme from Hb. Here we show using a combination of biophysical and structural methods that Shr uses its HIDs to selectively bind to the heme-loaded form of Hb, slowing the rate of heme release by directly contacting the edges of its protoporphyrin rings. However, receptor dynamics within the Shr–Hb complex act to transiently uncap the HIDs from Hb's β subunit, enabling heme's gated release and subsequent capture by the receptor. This "cap and release" mechanism exploits the β subunit's inherent weaker affinity for heme (26), allowing *S. pyogenes* to preferentially capture only heme-saturated forms of Hb that contain iron.

Results

Shr Preferentially Recognizes Holo-Hb by Capping Its Heme Molecules. To gain insight into how Shr uses its unusual HIDs to engage Hb, we determined the crystal structure of HID2 bound

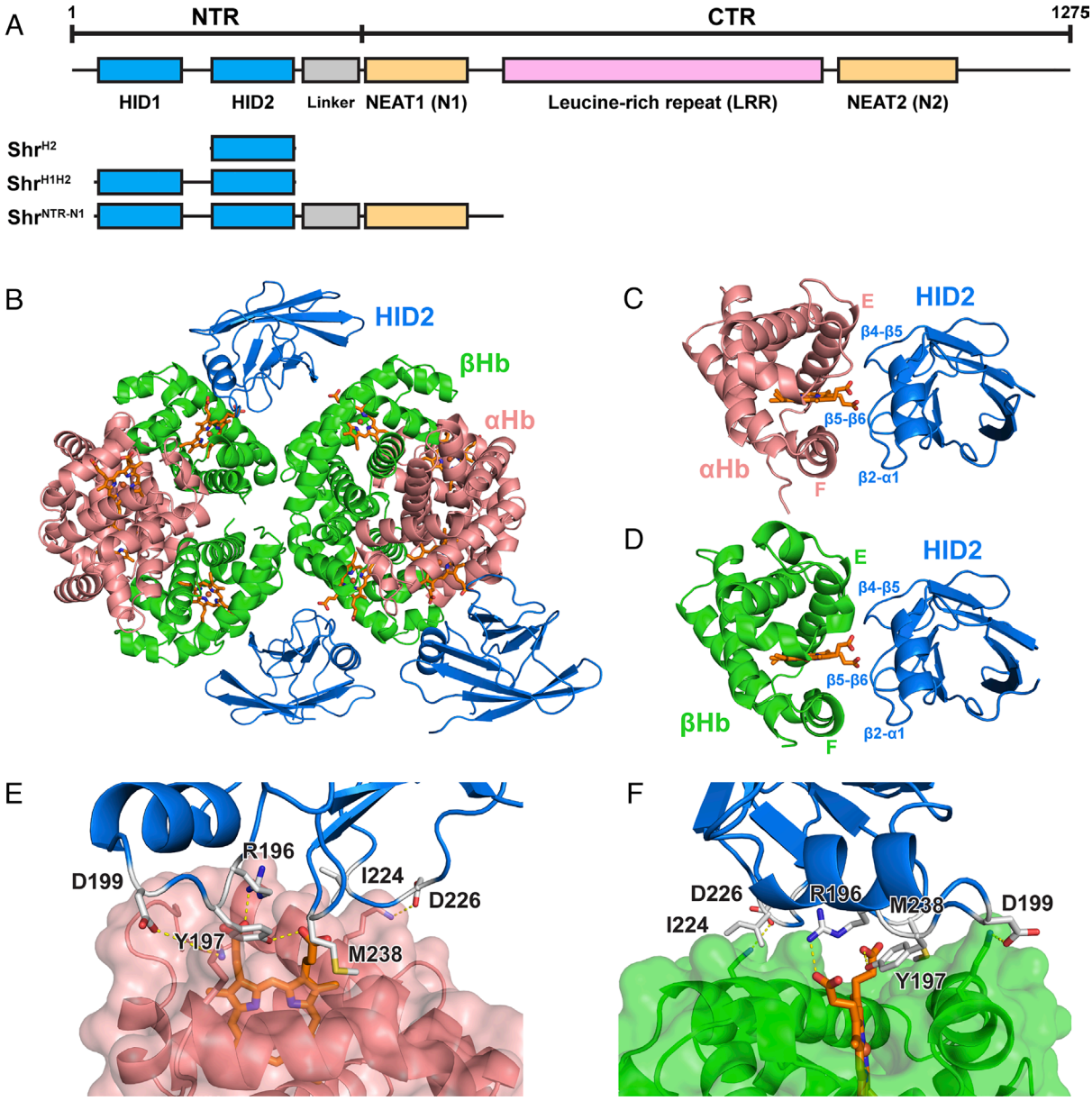

Fig. 1. Structure of the Hb–Shr^{H2} complex. (*A*) Domain schematic of the Shr receptor. The polypeptide constructs used in this study are shown below. (*B*) Crystal structure of the Hb–Shr^{H2} complex. The asymmetric unit of the crystal contains two tetramers of Hb that are bound by three molecules of Shr^{H2}. (*C* and *D*) HID2 binds over the heme pockets in both the α and β chains of Hb. These capping interactions directly contact both the heme and globin chain, burying an average of ~153 Å^2 and ~408 Å^2 of solvent-accessible surface area, respectively. Hb contacts originate from three surface loops in HID2: β2-α1, β4-β5, and β5-β6. (*E*) Expanded view of the Hb-receptor interface showing interactions with the heme molecule bound to the α subunit. The heme molecules are shown in stick format with oxygen and nitrogen atoms colored red and blue, respectively. Side chains in the receptor that interact with Hb are shown in stick format. (*F*) Identical to panel (*E*), except that receptor contacts to the β subunit in Hb are shown. Hb is in its ferric form. Color scheme: α subunit (salmon), β subunit (green), and HID2 (blue).

to methemogloin [metHb, the ferric form of Hb thought to predominate outside the red blood cell (RBC)] at 2.1 Å resolution (Hb-Shr^{H2}, where Shr^{H2} corresponds to residues N175-Q285 of Shr) (Fig. 1*A* and *SI Appendix*, Table S1). The asymmetric unit contains well-defined electron density for two Hb tetramers that are bound to three HID2 modules (Fig. 1*B*). The HID2 proteins contact heme molecules located in both the α and β globin chains of Hb (αHb and βHb) by interacting with their solvent-projecting propionate moieties and adjacently positioned surface-exposed side chains in each globin's E- and F-helices. Each HID2 protein adopts a structurally unique Hb-binding fold that consists of a β-sandwich, which packs against a single α-helix. The edge of the stacked sheets containing the helix contacts Hb's heme pocket via residues located in three surface loops: β2-α1, β4-β5, and β5-β6 (Fig. 1 *C* and *D*). At both the αHb- and βHb-receptor interfaces, the side chains of residues R196 and Y197 in the β2-α1 loop of HID2 are positioned to donate hydrogen bonds to heme's propionate groups, and the aromatic ring of Y197 forms nonpolar interactions with a conserved leucine (F7) side chain located in Hb's F-helix (L86 and L91 in αHb and βHb, respectively) (Fig. 1 *E* and *F*). HID2's β5-β6 loop also contacts Hb residues that are adjacent to the heme molecule in each globin by positioning the side chain of M238 between hydrophobic residues located in their F-helices (A82, L83, and L86 in αHb, and T87, L88, and L91 in βHb). These primary interactions are supplemented by water-mediated hydrogen-bonding networks that connect Hb's E-helix to residues within HID2's β4-β5 and β5-β6 loops. Complex formation does not perturb the structure of HID2 or Hb, as the heavy atom backbone coordinates of Hb and HID2 in the complex can be superimposed to the coordinates of apo-HID2 (PDB: 6DKQ) and metHb (PDB: 6NBD) with rmsd values as small as 0.64 and 0.63 Å, respectively (further described in the *SI Appendix* section). Notably, human Hb in its ferric form exists in an equilibrium between tetrameric ($\alpha_2\beta_2$) and dimeric ($\alpha_1\beta_1$) states (the equilibrium constant is ~10 μM depending on solution conditions) (27, 28). As the heme-binding pockets in the dimer and tetramer are solvent exposed, HID2 can be expected to bind in a similar manner to both forms of Hb.

The importance of heme-capping interactions for receptor binding to Hb was investigated using targeted mutagenesis and NMR spectroscopy (Fig. 2). Adding unlabeled tetrameric Hb that is saturated with heme (holo-Hb) to [U-^{15}N] Shr^{H2} causes significant line broadening of its ^{1}H-^{15}N heteronuclear single-quantum coherence (HSQC) spectrum, consistent with Shr^{H2} forming a high molecular weight complex with Hb (compare Fig. 2 *A* and *B*) (19, 29). Interestingly, the heme-capping interactions observed in the crystal structure are essential for receptor binding, as only minimal spectral changes are observed when Hb lacking heme (apo-Hb) is added to [U-^{15}N] Shr^{H2} (compare Fig. 2 *A* and *C*). Similar titration experiments were formed using a labeled HID1 polypeptide and revealed that this domain also binds to the heme loaded form of Hb, but not to apo-Hb or holo-myoglobin (holo-Mb) (*SI Appendix*, Fig. S7). At the Hb concentrations used in the NMR experiments, holo-Hb is presumably tetrameric, while apo-Hb is expected to be a mixture of dimeric and monomeric Hb species (30). Nevertheless, the NMR data indicate that these lower molecular weight apo-Hb species do not bind to HID1 or HID2 with high affinity, since if they did, significant changes in their spectra would occur as a result

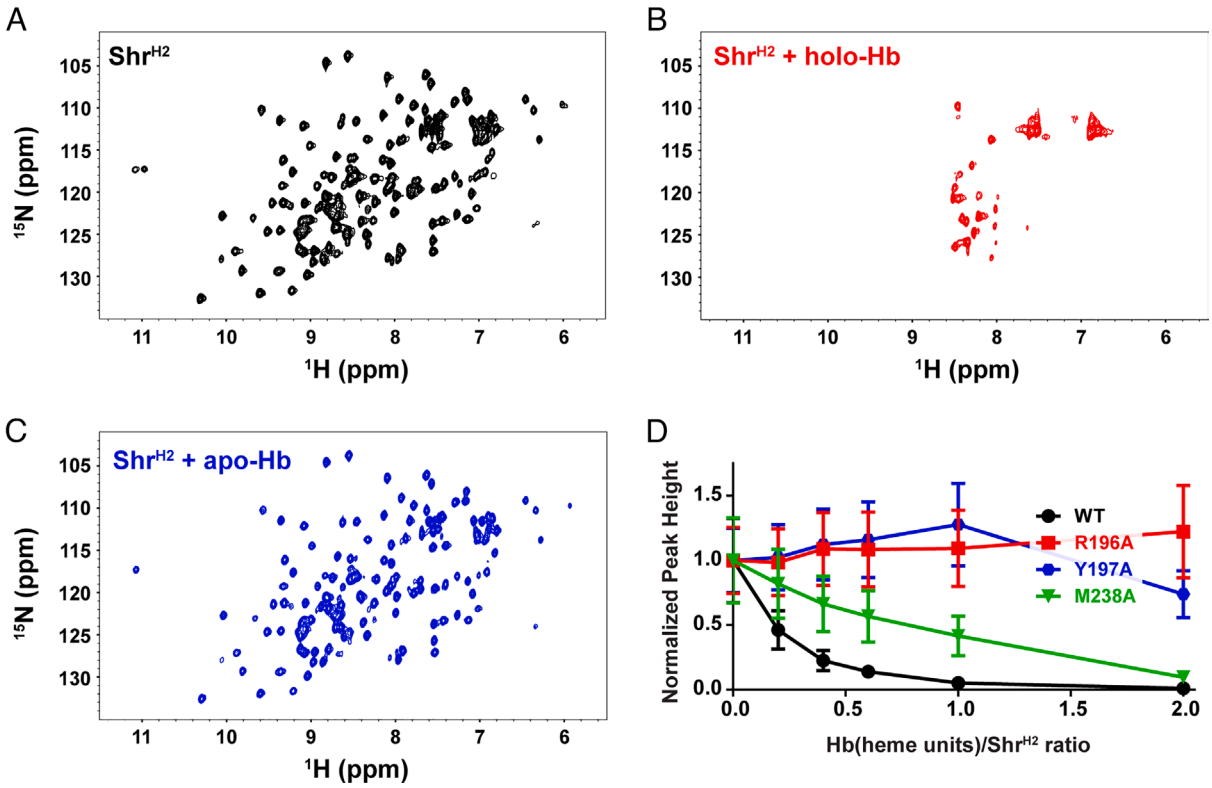

Fig. 2. HID2 preferentially interacts with holo-Hb. ^{1}H-^{15}N HSQC spectra shown for (*A*) [U-^{15}N] Shr^{H2} alone, (*B*) after the addition of fourfold molar excess heme-bound holo-Hb, and (*C*) after the addition of fourfold molar excess apo-Hb. Significant linewidth broadening is observed in *B* indicating that HID2 binds to holo-Hb, but negligible changes in the spectrum of Shr^{H2} are observed in *C* indicating that it does not bind to apo-Hb. (*D*) NMR-based Hb-binding assay for a series of Shr^{H2} variants containing alanine substitutions: R196A (red), Y197A (blue), and M238A (green). For each ^{15}N-labeled Shr^{H2} variant a series of ^{1}H-^{15}N HSQC spectra were recorded after adding varying amounts of heme-loaded Hb. The normalized peak heights of the NMR spectra are plotted as a function of Hb–Shr^{H2} ratio (varied from 0.25 to 2.0 when Hb is expressed in heme units). The data for the Y197A variant have been published previously (19). Error bars represent the SD of peaks selected for analysis.

of chemical exchange. To identify specific receptor-Hb interactions that contribute to binding affinity, a series of Shr^{H2} variants containing targeted alanine substitutions were tested for their ability to bind Hb (Fig. 2*D* and *SI Appendix*, Fig. S2). Only Shr^{H2} proteins harboring R196A or Y197A substitutions are significantly impaired in binding, indicating that their contacts to Hb's heme propionate groups are the main drivers of affinity. More modest effects occur when M238 (β5-β6 loop) is altered to disrupt interactions with the F-helices in αHb and βHb, while substitution of other globin-contacting residues in HID2 have little impact on binding (*SI Appendix*, Fig. S2). HID2-globin interactions may confer specificity for Hb, as Shr^{H2} does not bind with appreciable affinity to holo-Mb, a structurally related member of the globin family (*SI Appendix*, Fig. S1). Based on primary sequence homology, the related N-terminal HID1 module in the receptor is also expected to engage Hb's heme molecules. However, HID1 has significantly weaker affinity for Hb as compared with HID2 (K_D values of ~143 μM and 16 μM, respectively) (19), consistent with its primary sequence lacking a residue analogous to R196 in HID2 that is an important determinant for binding (R196 in HID2 is replaced by P54 in HID1). Thus, we conclude that the Shr receptor preferentially binds to the holo-form of Hb in a process which is primarily driven by heme-capping interactions that originate from its HID2 module.

Capping Interactions Enable the Receptor to Selectively Remove Heme from Hb's β Subunit. Native electrospray ionization mass spectrometry (ESI-MS) was used to track the process of receptor-mediated heme removal from Hb (31, 32). We investigated heme transfer to $Shr^{NTR\text{-}N1}$ (Shr, residues 26 to 550), which is the minimal unit within the receptor that is capable of capturing heme from Hb [$Shr^{NTR\text{-}N1}$ contains both HIDs, the linker domain, and the heme-binding NEAT1 domain (N1)] (Fig. 1*A*) (18). As expected, prior to encountering the receptor, holo-Hb at the concentrations used in the experiment exists in an equilibrium between its tetrameric ($\alpha_2\beta_2$) and dimeric ($\alpha_1\beta_1$) forms (Fig. 3*A* and *SI Appendix*, Fig. S3*A*) (30, 33). However, after mixing with an equimolar amount of apo-$Shr^{NTR\text{-}N1}$, 16.1 ± 0.9% of the receptor acquires heme from Hb within 15 min, which increases to 21.5 ± 3.4% and 27.9 ± 2.1% after 2 and 48 h, respectively (Fig. 3*B* and *SI Appendix*, Fig. S3*C*). Moreover, a population shift occurs from Hb tetramers toward stable $\alpha_1\beta_1$ dimers that remain either fully loaded with heme ($\alpha_1\beta_1{\cdot}2$) or have lost one of their heme molecules to $Shr^{NTR\text{-}N1}$ ($\alpha_1\beta_1{\cdot}1$). The finding that heme is only partially removed from Hb when the $Shr^{NTR\text{-}N1}$ receptor is present at limiting concentrations is expected, as the N1 domain has weaker binding affinity for heme as compared with Hb (26, 34). The rate of heme movement to the receptor is consistent with it occurring through a passive process in which it is first released from Hb into the solvent and

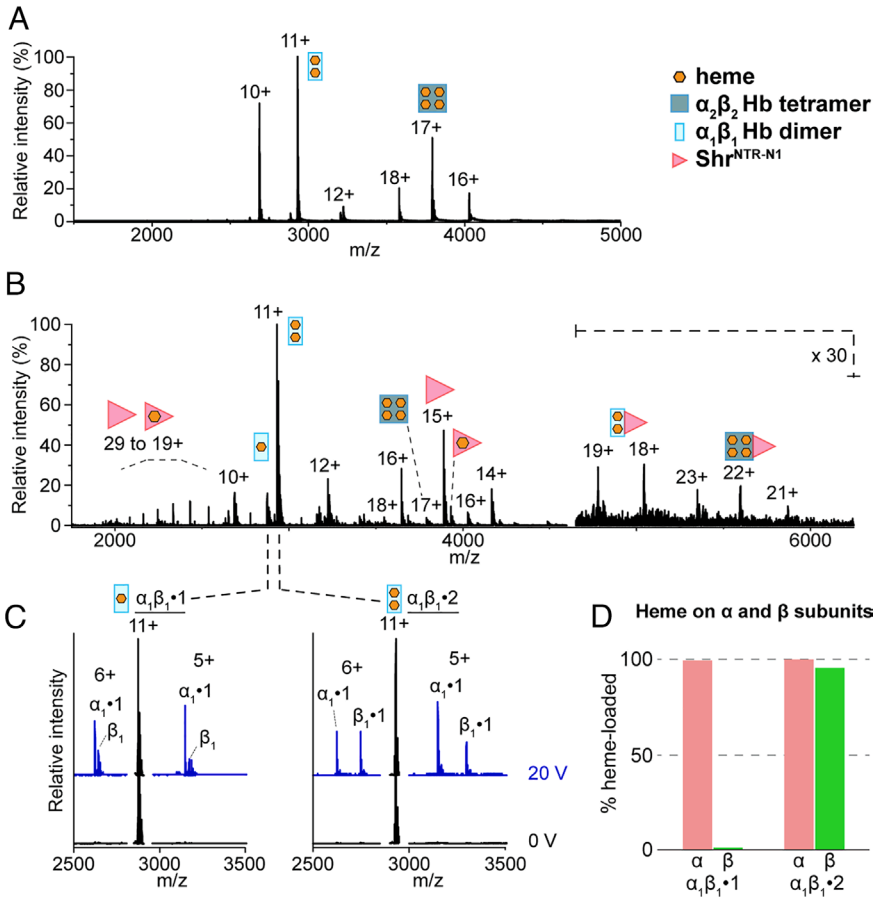

Fig. 3. $Shr^{NTR\text{-}N1}$ captures heme from the β subunit of Hb. Native mass spectrometry measurements showing heme transfer from Hb to $Shr^{NTR\text{-}N1}$. (*A*) Control experiment showing the raw native MS spectrum of 5 μM human Hb (in heme units). (*B*) Native MS spectrum acquired 2 h after mixing equimolar amounts of Hb and $Shr^{NTR\text{-}N1}$ (both at 5 μM). The signals of the high m/z range have been magnified 30-fold to improve their visibility. The highest intensity charge states and identities of the mass species are labeled. (*C*) HCD of dimeric forms of Hb generated after incubation with $Shr^{NTR\text{-}N1}$. The panels show the effect of collisional energy on the 11+ charge state of dimeric Hb containing a single heme molecule ($\alpha_1\beta_1{\cdot}1$) (*Left*) or dimeric Hb containing both of its hemes ($\alpha_1\beta_1{\cdot}2$) (*Right*). Both species were individually isolated in the gas phase and fragmented. At 20 V, the m/z region is magnified to view the fragmentation products (precursor at 0 V shown in black without magnification). These data demonstrate that the receptor initially removes heme from the βHb subunit. (*D*) A bar plot showing the percentage of heme-bound αHb and βHb subunits after 20 V HCD fragmentation. Data are for precursors of dimeric Hb containing either one ($\alpha_1\beta_1{\cdot}1$) or two ($\alpha_1\beta_1{\cdot}2$) heme molecules.

then subsequently captured by apo-Shr^{NTR-N1} (26). We wondered whether the receptor preferentially captured heme released from either the αHb or βHb subunits during the initial stages of the transfer reaction. To investigate this issue, the 11+ charge states of dimeric Hb species containing either one ($\alpha_1\beta_1$·1) or two ($\alpha_1\beta_1$·2) heme molecules were isolated and fragmented by higher-energy collisional dissociation (HCD; orbitrap mass spectrometer), which passes the gas-phase proteins through a collision cell filled with high pressure nitrogen at a specified collision energy. HCD was performed using a range of energies (0, 20, and 40 V) that were tuned to either disrupt globin-globin (20 V) or globin-heme interactions (40 V, *SI Appendix*, Fig. S3*D*). This analysis reveals that βHb within the $\alpha_1\beta_1$·1 species has lost its heme, while the majority of αHb subunits within the dimer remain bound to heme (Fig. 3 *C*, *Left* and *D*). The isolated $\alpha_1\beta_1$·2 dimer from the same sample retains a heme molecule in each subunit when fragmented at 20 V, which shows heme is not being displaced by the applied voltage (Fig. 3 *C*, *Right* and *D*).

To determine if the HIDs are responsible for Shr's ability to preferentially remove heme from the βHb subunit, their effects on the kinetics of heme release from Hb were determined using ultraviolet-visible (UV-Vis) spectrophotometry (Fig. 4). When the metHb form of Hb is rapidly mixed with a high affinity heme scavenger H64Y/V68F apomyoglobin (apo-Mb), biphasic time-dependent spectral changes are observed at 405 nm (A_{405}) which report on the rate of spontaneous heme release from Hb into the solvent and its subsequent capture by apo-Mb (26, 35, 36). The rapid and slow spectral changes are defined by k_{fast} and k_{slow} rate constants that have been shown to characterize heme loss from the βHb and αHb chains, respectively (26, 36). Interestingly, mixing Hb with a polypeptide that contains both of Shr's HIDs (Shr^{H1H2}, residues S26 to Q285) inhibits slow heme release from the αHb subunit, while faster spectral changes that are diagnostic for heme loss from βHb are only marginally affected; the presence of Shr^{H1H2} at saturating concentrations causes a modest ~threefold decrease in k_{fast}, while the slower process characterized by k_{slow} is eliminated (Fig. 4*A* and *SI Appendix*, Table S2). This finding suggests that the receptor's HIDs selectively gate heme release from Hb, blocking its egress from αHb while leaving βHb unaffected. This is further supported by measurements of the total heme transferred from Hb after 20 h, since it is progressively reduced to a final value of ~50% when saturating amounts of Shr^{H1H2} are added (Fig. 4*B* and *SI Appendix*, Table S2). Thus, we conclude from the ESI-MS and kinetics data that Shr^{NTR-N1} preferentially captures heme that is passively released from βHb, because its HIDs effectively block heme release from αHb.

Transient Uncapping by the Receptor Facilitates Heme Release from βHb. Analytical ultracentrifugation experiments indicate that two Shr receptors bind to a single Hb tetramer, suggesting that within the receptor–Hb complex Hb's heme molecules are capped by a HID (19). Based on the crystal structure, similar capping interactions are expected to occur for complexes formed at lower concentrations where dimeric forms of Hb predominate, but the receptor would bind to the dimer with 1:1 stoichiometry (30, 33). How then does Shr selectively capture heme from βHb? To explore this issue, we subjected the Hb–Shr^{H1H2} complex to size-exclusion chromatography coupled with small-angle X-ray scattering detection (SEC-SAXS). Molecular weight estimates obtained from small angle X-ray scattering (SAXS) and multiangle light scattering (MALS) are consistent with two Shr proteins binding to a Hb tetramer (the quaternary form of Hb that predominates at the concentrations used in this experiment)

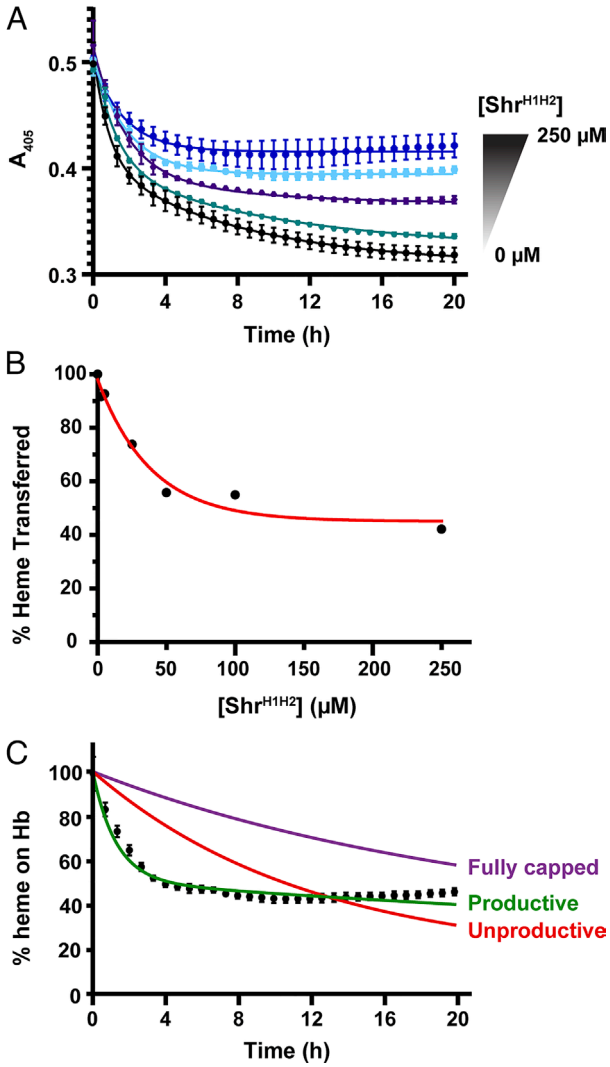

Fig. 4. Effects of HID binding on heme release from Hb. (*A*) Heme release experiments monitoring the transfer of heme from holo-Hb to apo-Mb in the presence and absence of Shr^{H1H2}. The plot shows the time-dependent changes in the Soret band absorbance at 405 nm after mixing holo-HbA with excess apo-Mb in the presence of 0 (black), 5 (blue-green), 25 (purple), 100 (light blue), or 250 μM Shr^{H1H2} (dark blue). Lines represent fitting of the data to an exponential decay and error bars represent the SD of three replicates. Increasing the amount of Shr^{H1H2} reduces both the rate and amount of heme that is transferred. Control experiments confirm that the absorbance changes are caused by heme release from Hb and are not a result of Shr^{H1H2} binding to either Hb or Mb (*SI Appendix*, Fig. S4). Shr^{H1H2} also binds to the carbonmonoxy form of Hb (HbCO), but because HbCO releases heme very slowly we have not determined if this process is slowed by the HID modules. (*B*) Percentage of heme lost from Hb as a function of the concentration of Shr^{H1H2}. The change in absorbance in panel *A* at 405 nm measured 20 h after mixing was used to determine the amount of heme transferred. Error bars corresponding to values determined by propagation of uncertainty are present, but they are too small to be visible at this scale. At saturating Shr^{H1H2} concentrations, only ~50% of Hb heme molecules are transferred to apo-Mb. This is consistent with full capping of half of the heme molecules in Hb. (*C*) Graph showing the time-dependent change in the percentage of heme remaining on Hb in the presence of 100 μM Shr^{H1H2} (black spheres) and its agreement with different kinetic models describing the effects of HID capping on heme release from Hb. The time course was modeled assuming formation of either a: i) "fully capped" Hb–Shr^{H1H2} complex in which the HIDs do not detach from Hb (purple), ii) "unproductive" complex in which the receptor is positioned to enable the weakly binding HID1 module to detach from αHb (red), and iii) a productive complex in which the receptor is positioned such that the weakly binding HID1 module detaches from βHb (green). Only models assuming formation of the productive complex adequately recapitulate the experimental data. Notably, at ~20 h more than 50% of Hb's heme is released in the unproductive binding model. This is because a small fraction Hb is not bound by the receptor (K_D = 16 μM), which enables heme release from βHb in addition to αHb. The kinetic models are described in the *SI Appendix*.

(30, 33). However, in silico models that assume formation of only a closed Hb–receptor complex in which both HID1 and HID2 are fully bound to Hb's heme molecules are not compatible with the scattering data. This closed structure is too compact because it has a predicted D_{max} value of ~120 Å, whereas the D_{max} calculated from the SAXS data is 172 Å (Fig. 5*A*). Because HID1 has very weak affinity for Hb, we reasoned that it could detach from Hb, thereby creating an expanded structure. Indeed, the experimental SAXS data are well fit (χ^2 = 1.16) by a two-state ensemble model of the complex in which HID2 remains affixed to Hb, while HID1 adopts either closed (Hb bound) or open (Hb disengaged) states that have relative populations of ~36% and ~64%, respectively (Fig. 5*B* and *SI Appendix*, Fig. S5*D*). The notion that HID1 transiently engages Hb's heme is consistent with the results of heme release experiments using polypeptides that contain the isolated HID modules, as the HID2 blocks heme release from Hb to greater extent than HID1 (*SI Appendix*, Fig. S8). To determine if dynamic binding by HID1 in the complex could explain the experimental transfer data (Fig. 4), a kinetic model of this process was constructed using the previously determined rate constants for heme binding and spontaneous release from Hb and Mb, as well as the measured HID-Hb-binding affinities (*SI Appendix*). The best agreement with both the transfer kinetics and SAXS data occurs when the receptor is presumed to form a dynamic "productive" complex with Hb in which HID2 completely caps αHb, while the HID1 module adopts open and closed states over βHb's heme with populations similar to those predicted by the SAXS data (Fig. 5*C*). Importantly, poor agreement with the transfer data occurs if it is assumed the receptor adopts a static conformation in which its HID1 module either continuously caps (Fig. 4*C*, purple) or stays disengaged from βHb's heme molecule. Moreover, the experimental data are not well fit if the receptor is assumed to bind to Hb in a reversed orientation such that its HID1 module can transiently disengage from the αHb instead of the βHb subunit (Fig. 4*C*, red). This binding orientation is not productive for transfer, since αHb releases heme too slowly from Hb even when it is fully uncapped by HID1. More detailed modeling of the kinetics data suggests that Shr can still effectively remove heme from Hb even when it binds promiscuously to Hb to form both productive (HID1 over βHb) and nonproductive (HID2 over βHb) complexes (*SI Appendix*, Fig. S6*A*). However, only models that assume no more than ~20% of the receptors engage Hb nonproductively adequately fit the experimental heme transfer data, as well as the SAXS-derived constraint that ~64% of the HID1 modules in the bound receptor adopt an open, disengaged state (*SI Appendix*, Fig. S6*B*). Thus, we conclude the primary path for heme transfer to the receptor occurs via the dynamic complex shown in Fig. 5*C* in which motions within its HID1 module enable gated heme release from the βHb subunit.

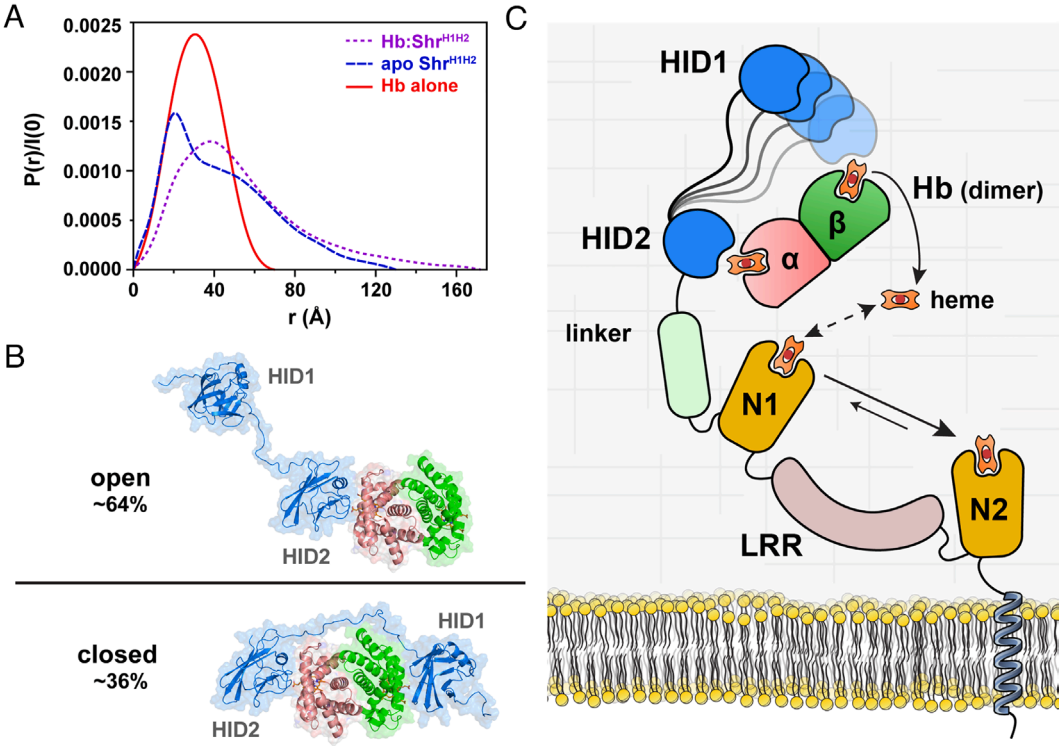

Fig. 5. SAXS experiments indicate the Hb–Shr complex is dynamic. (*A*) Distance distribution function P(r) calculated from SAXS data obtained for: Hb (red), Shr^{H1H2} (blue), and the Hb–Shr^{H1H2} complex (purple). (*B*) SAXS-derived ensemble model of the productive Hb–Shr^{H1H2} complex showing a single Shr^{H1H2} protein engaging the Hb dimer. In the productive complex HID2 within the Shr^{H1H2} protein is bound to αHb like the crystal structure, and HID1 adopts two possible conformations: i) an "open" conformer in which HID1 is dissociated, and ii) a "closed" compact conformer in which HID1 is positioned near the heme molecule in βHb. The image was generated from complex models that assumed two Shr^{H1H2} proteins bound to a Hb tetramer. More complex three-state ensemble models of the complex also agree with the SAXS data and predict similar populations for the open and closed states of HID1 (*SI Appendix*, Fig. S5 *C* and *D*). For clarity, binding of one receptor to a Hb dimer is shown. (*C*) The cap and release mechanism describing Shr-mediated heme removal from dimeric Hb. The full-length Shr protein is embedded in the lipid bilayer of the bacterial cell via its C-terminal transmembrane helix. The HID1 and HID2 modules located within its NTR cap the heme molecules located in the β and α subunits of dimeric Hb, respectively. The weakly bound HID1 module transiently disengages from the heme-binding pocket on the β subunit enabling heme release and subsequent capture by N1. Heme released from Hb may also be directly captured by the N2 NEAT domain, but this likely occurs less frequently as N2 is expected to be positioned farther away from Hb. Overall net heme flow to the N2 NEAT domain presumably occurs because of its higher affinity for heme. Note, in panels *B* and *C* Hb is shown in its dimeric form which predominates when Hb is diluted after RBC lysis (30, 33). Based on our crystal structure of the Hb–Shr^{H2} complex (Fig. 1) and native mass spectrometry studies of the Hb–$Shr^{NTR\text{-}N1}$ complex (Fig. 3) a similar mode of receptor binding to tetrameric forms of Hb is expected, except that Shr would bind with 2:1 stoichiometry.

Discussion

To gain access to iron during infections *S. pyogenes* uses the Shr receptor to capture human Hb released from lysed RBCs (18, 37). Shr is located on the microbial surface and binds to Hb and captures its heme molecules using an N-terminal segment that contains two structurally unique HID modules connected via an ordered linker to a heme-binding N1 NEAT domain (the NTR-N1 region) (18, 19). This unit is followed by LRR and heme-binding N2 NEAT domains, and a C-terminal transmembrane helix that embeds Shr into the membrane. Shr's multidomain architecture is conserved in other streptococci and clostridia receptors, but how it binds Hb and captures its heme remains poorly understood. Our results indicate that Shr forms a dynamic complex that enables it to selectively recognize only the heme-loaded form of Hb. A crystal structure of the Hb–Shr^{H2} complex and binding experiments reveal that Shr uses its HID2 module to engage Hb via its heme molecules (Fig. 1). Residues R196 and Y197 within HID2's β2-α1 loop mediate heme-capping interactions and are the most significant contributors to binding affinity, while HID2 contacts to residues in the globin E- and F-helices likely confer binding selectivity for Hb (Fig. 2 and *SI Appendix*, Fig. S1). Based on primary sequence homology and NMR experiments (*SI Appendix*, Fig. S7), Shr's HID1 module is also expected to cap Hb's heme molecules via a similar mechanism, but these interactions are much weaker because it lacks a key propionate-contacting arginine residue (19). Recently, another structure of the Hb–Shr^{H2} complex was deposited in the Protein Data Bank (PDB: 7CUE,38) and is in agreement with the binding mode reported here. Shr has been shown to bind to heme-loaded Hb and to the $\alpha_1\beta_1$Hb–Hp complex (17). Our structural and biochemical data further show that HID-mediated heme contacts confer selectivity for holo-Hb in both its tetrameric and heterodimeric forms (Figs. 1–3 and *SI Appendix*, Fig. S7). Shr can discern holo-Hb from other hemoproteins, as both HID1 and HID2 do not interact with heme-loaded Mb to an appreciable extent (*SI Appendix*, Figs. S1*B* and S7*D*). This selectivity is presumably advantageous, as it ensures that *S. pyogenes* only binds iron-rich forms of Hb, while avoiding interactions with other hemoproteins that may be less prone to release their heme.

Our results suggest that the Shr receptor uses a cap and release mechanism to gather heme from Hb. Once outside RBCs, Hb is significantly diluted and dissociates into free heterodimers ($\alpha_1\beta_1$Hb) in which its heme molecules are oxidized (30, 33). ESI-MS experiments indicate that Shr's N-terminal heme removal unit ($Shr^{NTR\text{-}N1}$) binds to $\alpha_1\beta_1$Hb heterodimers and preferentially removes heme from their βHb subunits (Fig. 3). This is accomplished by first engaging the heme molecules within holo-Hb using the receptor's HID1 and HID2 modules, which form capping interactions that can slow heme release (Fig. 4). However, SAXS data indicate that the receptor–Hb complex is dynamic and is consistent with Shr's weaker binding HID1 module being able to transiently disengage from Hb's heme (Fig. 5). Both the SAXS and heme transfer data are well described by kinetic models in which the receptor forms a dynamic productive complex with Hb where its HID2 module masks the heme molecule bound to αHb limiting its release, while HID1 transiently unlatches from βHb to allow its heme to be transferred to Shr's N1 domain (Fig. 5*C*). This binding mode exploits the greater propensity of βHb to release its heme and agrees best with the experimental data when ~64% of the population of complexes have their HID1 modules disengaged from the αβ heterodimers. Only formation of this dynamic productive complex can effectively remove heme from Hb, as kinetic modeling of alternative complexes in which the receptors adopt either static structures or bind in a reverse orientation (HID1 and HID2 bound to αHb and βHb, respectively) are predicted to be less effective at gathering heme from Hb (Fig. 4*C*). A similar mode of heme removal presumably occurs at higher protein concentrations that cause Hb to tetramerize, but two Shr receptors would bind to the two αβ heterodimer units within the $\alpha_2\beta_2$ tetramer. Heme captured by N1 is then transferred to a high-affinity heme-binding N2 NEAT domain located at Shr's C-terminus for storage, or to the Shp hemoprotein for transit across the peptidoglycan and import into the cell (39, 40). The cap and release mechanism may also be operative on the $\alpha_1\beta_1$Hb-Haptoglobin(Hp) complex that directs Hb for removal from circulation via CD163-mediated macrophage clearance. This is because *S. pyogenes* has been shown to bind the $\alpha_1\beta_1$Hb–Hp complex and use it as iron source (17, 41), while the atomic structure of the $\alpha_1\beta_1$Hb–Hp complex reveals that the Shr-binding and Hp-binding surfaces on Hb are distinct and should not obstruct each other (42, 43). However, as the $\alpha_1\beta_1$Hb–Hp complex releases heme very slowly, it is possible that its heme needs to be removed on the cell surface through an active process whose mechanism remains to be elucidated (44, 45). Shr also binds to the ECM fibronectin and laminin glycoproteins (15, 16, 18), but since these interactions are primarily mediated by Shr's C-terminal NEAT2 domain, it seems unlikely that they will impair Shr's ability to capture heme from Hb (18). Beyond enabling the gated release process that is important for heme capture, bivalent binding by the HIDs is expected to promote binding avidity. This could be advantageous as it would increase the lifetime of Hb molecules that are bound to the microbial cell surface and thereby facilitate removal of their heme molecules by Shr or as a result of Hb degradation by bacterial proteases as has been observed in other microbial species (46–48). Avidity increases the lifetime of the receptor–Hb complex, since Hb will not completely dissociate from the receptor when only one of the two HID modules detaches. Moreover, in this partially detached state, the dissociated HID module can exhibit a higher local concentration near Hb, increasing its reassociation rate and thereby its effective affinity (49, 50).

The molecular strategy used by *S. pyogenes* to remove heme from Hb is distinct from previously characterized mechanisms used by other microbial pathogens. Three types of microbial Hb receptors have been identified: i) the surface displayed IsdB/IsdH receptors from *S. aureus* (51–56), ii) outer membrane-associated HpuA receptors in gram-negative bacteria such as *Kingella denitrificans* (57, 58), and iii) surface displayed Hb–Hp receptors (HpHbR) present in the pathogenic trypanosomes *Trypanosoma brucei* and *Trypanosoma congolense* (59–61). These receptors are structurally distinct, but like Shr, the trypanosomal HpHbR receptors preferentially capture heme-loaded Hb by directly contacting its heme's propionate groups using a combination of tyrosine and cationic residues (59, 60). However, these capping interactions only occur at the βHb subunit and presumably fulfill a distinct functional purpose by selectively blocking the release of its labile heme molecule until the entire Hp–Hb complex can be internalized and degraded within the lysosome to gain access to its heme. The other microbial receptors do not appear to selectively recognize holo-Hb. However, similar to Shr, gram-negative bacteria may also exploit the βHb subunit's greater propensity to release its heme, since in the Hb–HpuA complex the βHb heme pocket is thought to be positioned near the membrane-embedded transporter that imports released heme into the cell (57, 58, 62). Interestingly, the domain architectures of the Shr and staphylococcal IsdB/IsdH Hb receptors are strikingly similar, as each gathers heme from Hb using a multidomain unit in which an

N-terminal Hb-binding domain is connected via a structured helical linker to a heme-binding NEAT domain (53–55). However, the mechanisms used by these receptors to capture heme from Hb are radically different. In Shr, the N-terminal HIDs transiently cap Hb's heme molecules modulating the rate at which heme is spontaneously released from the βHb subunit. In contrast, the IsdB/IsdH receptors use a distinct N-terminal NEAT domain to engage each globin at a site that is distal to the heme molecule, and then employ a C-terminal NEAT domain to distort the Hb-heme binding pocket and extract heme (36, 63–65). Presumably, these distinct heme acquisition mechanisms result from differences in specific iron needs, immunological avoidance mechanisms, and ecological niches of these related gram-positive pathogens. *S. pyogenes* strikes a balance that maximizes heme flow into the cell, preferentially recognizing the heme-bound form of Hb, while nevertheless retaining the ability to scavenge labile heme located within Hb's β subunit. Future studies will need to be focused on learning how heme is bound by the Shr NEAT domains and transferred to other components in the uptake system, as well as the role of additional domains like the LRR in the extraction process. This work promises to reveal how pathogens acquire nutrients during infections and could facilitate the development of new therapeutics that limit microbial access to iron.

Materials and Methods

Purification of Shr, Hb, and Myoglobin. Recombinant Shr protein constructs were expressed in *Escherichia coli* and purified using standard methods as previously described (19). Human Hb was prepared from the blood of a healthy donor provided by the CFAR Virology Core Lab at the UCLA AIDS Institute, purified in the carbonmonoxy form (HbCO), and converted to oxidized metHb as previously described (36). H64Y/V68F myoglobin (apoMb) was expressed recombinantly and purified as previously described (36). Further details are described in *SI Appendix, Materials and Methods*.

X-Ray Crystallography. Purified Shr^{H2} and metHb were combined in a 2:1 ratio at a concentration of 45 mg/mL, leading to crystal formation in a solution of 11% PEG-6000, 240 mM lithium chloride, 100 mM sodium acetate, pH 5.0. Crystals were transferred to a cryoprotectant solution containing 20% glycerol and flash frozen at 100 K. Data were collected at the Advanced Photon Source on beamline 24-ID-C on a DECTRIS-PILATUS 6M detector and processed using the X-ray Detector Software (XDS) package (66). The structure was solved using molecular replacement with PHASER (using models PDB: 6DKQ and PDB: 1IRD) and refined to 2.1 Å using Coot and BUSTER (19, 67–69). Coordinates and structure factors have been deposited in the Protein Data Bank under PDB ID 8DOV. Complete statistics are presented in *SI Appendix*, Table S1. Additional details about crystallization, molecular replacement, and refinement are described in *SI Appendix, Materials and Methods*.

NMR Spectroscopy. Shr proteins were dialyzed against 50 mM NaH_2PO_4/Na_2HPO_4 pH 6.8, 100 mM NaCl. Buffer-matched Hb in the carbonmonoxy form was titrated into the samples to make Hb(heme basis):Shr^{H2} at the following ratios: 0:1, 0.2:1, 0.4:1, 0.6:1, 1:1, and 2:1. For the apo-Hb:HID experiments, heme-free Hb (apo-Hb) was prepared as previously described and added to Shr^{H1} or Shr^{H2} at a 4:1 ratio (70–72). For the holo-Mb experiments with Shr^{H1} and Shr^{H2}, the holo form of myoglobin (holo-Mb) was purchased from Sigma-Aldrich and further purified by gel-filtration chromatography with a Superdex S75 size-exclusion column prior to addition to Shr^{H1} or Shr^{H2}. An ^{1}H-^{15}N HSQC spectrum was recorded at each titration point. NMR experiments were performed at 298K on Bruker DRX 500 and 600 MHz spectrometers equipped with triple resonance cryogenic probes. NMR spectra were processed using NMRPipe and TopSpin 3.5 (Bruker BioSpin) and analyzed using NMRFAM-SPARKY (73, 74). Resonances arising from disordered regions of the protein were excluded from quantification.

Kinetics of Heme Dissociation from Hb. Purified metHb, $apoMb^{H64Y/V68F}$, Shr^{H1H2}, Shr^{H1}, and Shr^{H2} were buffer matched in 20 mM NaH_2PO_4/Na_2HPO_4 pH 7.5, 150 mM NaCl, and 450 mM sucrose. Shr^{H1H2} at a concentration of 0, 2.5, 5, 25, 50, 100, or 250 μM was mixed with 50 μM apo-Mb in a 384-well plate, and heme transfer reactions were initiated by injecting metHb to a final concentration of 5 μM on a heme basis in a SpectraMax iD3 plate reader (Molecular Devices). The change in absorbance at 405 nm was measured every 2.5 min for 20 h. Shr^{H1} and Shr^{H2} at concentrations of 0 and 250 μM were mixed with 50 μM apo-Mb in a 384-well plate, and reactions performed and monitored as with Shr^{H1H2}. Experiments were performed in triplicate and the resulting curves were fit to either a two-phase or one-phase exponential decay equation in GraphPad Prism version 9.3.1 (GraphPad Software).

ESI-MS of Heme Transfer. Heme transfer reactions were analyzed by native nano-ESI-MS to quantitatively resolve apo- and holo- forms of heme-binding proteins. Hb and $Shr^{NTR\text{-}N1}$ were individually dialyzed into 50 mM ammonium acetate, pH 7.0. Reaction mixtures were initiated by diluting Hb to 5 μM and subsequently adding $Shr^{NTR\text{-}N1}$ to reach a 1:1 molar ratio. Replicates were created from independent reaction mixtures. Samples were analyzed after the desired time by loading 2 to 4 μL of sample into a platinum-coated pulled-glass capillary nano-ESI emitter tip and spraying on a Q Exactive UHMR Hybrid Quadrupole-Orbitrap mass spectrometer (Thermo Scientific). Spray voltage was set between 0.4 and 1.8 kV, ion transfer and detection optics were tuned for low m/z region (less than 15,000 m/z), the capillary temperature was set to 200 °C, and all spectra were collected either at 6,250 or 12,500 (at m/z 400) resolution. The percentage of heme-loaded $Shr^{NTR\text{-}N1}$ was quantified by dividing the sum of holo-protein peak intensities by the sum of holo- and apo-protein peak intensities.

HCD fragmentation on the 11+ charge states of $\alpha_1\beta_1{\cdot}1$ and $\alpha_1\beta_1{\cdot}2$ was performed by isolating the desired peak with a 20 m/z isolation window centered at m/z 2,874 and 2,931, respectively. Collisional energy was initially ramped from 10 to 40 V in increments of 10 on the isolated 11+ $\alpha_1\beta_1{\cdot}2$ charge state to find a voltage that would allow for subunit dissociation while keeping the heme ligand bound; this was found to be 20 V. Deconvoluted masses for each spectrum were generated using UniDec after manually removing the precursor ion, which otherwise caused errors in deconvolution (75). The percent of heme-loaded αHb and βHb globins released from HCD fragmentation was determined from the deconvoluted spectrum peak intensities.

SAXS. Samples of lone HbCO, lone Shr^{H1H2}, and Shr^{H1H2} incubated with HbCO at 2:1 ratio were submitted to the SIBYLS beamline (Advanced Light Source beamline 12.3.1, Lawrence Berkeley National Laboratory) at a total protein concentration of 10 mg/mL (76). SEC-SAXS was performed using an Agilent 1290 high-pressure liquid chromatography (HPLC) system with a Shodex KW-803 column equilibrated in size exclusion buffer (20 mM sodium phosphate, 150 mM NaCl, pH 7.2), and elution of analyte proteins at a flow rate of 0.65 mL/min. X-ray scattering was observed continuously using a Dectris PILATUS3 X 2M detector with collection in 2-s frames and an X-ray wavelength of 1.216 Å, with sample-to-detector distance of 2.0 m. Orthogonal detection of MALS, quasi-elastic light scattering, and refractometry allowed estimation of molecular weight using the ASTRA software package (Wyatt). SAXS frames from before and after the elution of protein were used to subtract the scattering contribution of buffer, and frames corresponding to the sample of interest were merged using ScÅtter IV (www.bioisis.net). Further processing including Guinier analysis and distance distribution calculations was performing using BioXTAS RAW and the ATSAS Suite (77, 78). A minimal ensemble search procedure was performed using the BILBO-MD service to describe the possible conformational ensembles sampled by the apo Shr^{H1H2} and Hb–Shr^{H1H2} complex, with the search models derived from AlphaFold2 predictions and restrained relative to each other as described in further detail in *SI Appendix, Materials and Methods* (79).

Data, Materials, and Software Availability. X-ray diffraction data have been deposited in Protein Data Bank (8DOV) (80).

ACKNOWLEDGMENTS. We thank Dr. Kat Ellis–Guardiola for useful discussions and advice. This work was funded by grants from the NIH R01AI052217, R01AI161828, and R01GM103479. R.M. was supported by National Institutes of Health Cellular and Molecular Biology Training Grant, Ruth L. Kirschstein NRSA GM007185. J.S. is funded by a NIH NIGMS-funded predoctoral fellowship (T32 GM136614). J.F. is also funded by a NIH NIGMS-funded predoctoral fellowship (T32 GM145388). A.K.G. acknowledges support from the National Institute of Dental and Craniofacial Research (T90 DE030860). We also acknowledge NIH equipment grants S10OD025073 and S10OD016336

for partial support of the NMR core facilities. The X-ray diffraction experiments were performed at the Northeastern Collaborative Access Team beamlines, which are funded by the National Institute of General Medical Sciences from the NIH (P30 GM124165). The research used resources of the Advanced Photon Source, a U.S. DOE Office of Science User Facility operated for the DOE Office of Science by Argonne National Laboratory under Contract number DE-AC02-06CH11357. SAXS data were collected at SIBYLS which is supported by the DOE-BER IDAT DE-AC02-05CH11231 and NIGMS ALS-ENABLE (P30 GM124169 and S10OD018483).

Author affiliations: [a]Department of Chemistry and Biochemistry, University of California, Los Angeles, CA 90095; [b]University of California, Los Angeles-United States Department of Energy Institute of Genomics and Proteomics, University of California, Los Angeles, CA 90095; and [c]Molecular Biology Institute, University of California, Los Angeles, CA 90095

1. N. L. Parrow, R. E. Fleming, M. F. Minnick, Sequestration and scavenging of iron in infection. *Infect. Immun.* **81**, 3503–3514 (2013).
2. H. Contreras, N. Chim, A. Credali, C. W. Goulding, Heme uptake in bacterial pathogens. *Curr. Opin. Chem. Biol.* **19**, 34–41 (2014).
3. C. Wandersman, P. Delepelaire, Heme-delivering proteins in bacteria. *Handb. Porphyr. Sci.* **26**, 191–222 (2014).
4. L. Ma, A. Terwilliger, A. W. Maresso, Iron and zinc exploitation during bacterial pathogenesis. *Metallomics* **7**, 1541–1554 (2015).
5. J. R. Sheldon, D. E. Heinrichs, Recent developments in understanding the iron acquisition strategies of gram positive pathogens. *FEMS Microbiol. Rev.* **39**, 592–630 (2015).
6. J. E. Choby, E. P. Skaar, Heme synthesis and acquisition in bacterial pathogens. *J. Mol. Biol.* **428**, 3408–3428 (2016).
7. J. R. Sheldon, H. A. Laakso, D. E. Heinrichs, Iron acquisition strategies of bacterial pathogens. *Microbiol. Spectr.* **4,** 1–32 (2016).
8. W. Huang, A. Wilks, Extracellular heme uptake and the challenge of bacterial cell membranes. *Annu. Rev. Biochem.* **86**, 799–823 (2017).
9. B. S. Conroy, J. C. Grigg, M. Kolesnikov, L. D. Morales, M. E. P. Murphy, Staphylococcus aureus heme and siderophore-iron acquisition pathways. *Biometals* **32**, 409–424 (2019).
10. J. R. Carapetis, A. C. Steer, E. K. Mulholland, M. Weber, The global burden of group A streptococcal diseases. *Lancet Infect. Dis.* **5**, 685–694 (2005).
11. A. P. Ralph, J. R. Carapetis, *Group A Streptococcal Diseases and Their Global Burden* (Springer, Berlin Heidelberg, 2012), pp. 1–27, 10.1007/82_2012_280.
12. M. J. Walker *et al.*, Disease manifestations and pathogenic mechanisms of group A Streptococcus. *Clin. Microbiol. Rev.* **27**, 264–301 (2014).
13. N. N. Lynskey, R. A. Lawrenson, S. Sriskandan, New understandings in Streptococcus pyogenes. *Curr. Opin. Infect. Dis.* **24**, 196–202 (2011).
14. J. A. Tsatsaronis, M. J. Walker, M. L. Sanderson-Smith, Host responses to group A Streptococcus: Cell death and inflammation. *PLoS Pathog.* **10**, e1004266 (2014).
15. M. Fisher *et al.*, Shr is a broad-spectrum surface receptor that contributes to adherence and virulence in group A Streptococcus. *Infect. Immun.* **76**, 5006–5015 (2008).
16. S. Dahesh, V. Nizet, J. N. Cole, Study of streptococcal hemoprotein receptor (Shr) in iron acquisition and virulence of M1T1 group A streptococcus. *Virulence* **3**, 566–575 (2012).
17. C. S. Bates, G. E. Montanez, C. R. Woods, R. M. Vincent, Z. Eichenbaum, Identification and characterization of a Streptococcus pyogenes operon involved in binding of hemoproteins and acquisition of iron. *Infect. Immun.* **71**, 1042–1055 (2003).
18. M. Ouattara *et al.*, Shr of group A streptococcus is a new type of composite NEAT protein involved in sequestering haem from methaemoglobin. *Mol. Microbiol.* **78**, 739–756 (2010).
19. R. Macdonald, D. Cascio, M. J. Collazo, M. Phillips, R. T. Clubb, The Streptococcus pyogenes Shr protein captures human hemoglobin using two structurally unique binding domains. *J. Biol. Chem.* **293**, 18365–18377 (2018).
20. T. K. Nygaard *et al.*, The mechanism of direct heme transfer from the streptococcal cell surface protein Shp to HtsA of the HtsABC transporter. *J. Biol. Chem.* **281**, 20761–20771 (2006).
21. M. Liu, B. Lei, Heme transfer from streptococcal cell surface protein Shp to HtsA of transporter HtsABC. *Infect. Immun.* **73**, 5086–5092 (2005).
22. N. Akbas *et al.*, Heme-bound SiaA from Streptococcus pyogenes: Effects of mutations and oxidation state on protein stability. *J. Inorg. Biochem.* **158**, 99–109 (2016).
23. M. Ouattara *et al.*, Kinetics of heme transfer by the Shr NEAT domains of group A Streptococcus. *Arch. Biochem. Biophys.* **538**, 71–79 (2013).
24. Y. S. Huang, M. Fisher, Z. Nasrawi, Z. Eichenbaum, Defense from the group A Streptococcus by active and passive vaccination with the streptococcal hemoprotein receptor. *J. Infect. Dis.* **203**, 1595–1601 (2011).
25. N. Chatterjee *et al.*, Native human antibody to Shr promotes mice survival after intraperitoneal challenge with invasive group A Streptococcus. *J. Infect. Dis.* **223**, 1367–1375 (2021).
26. M. S. Hargrove, T. Whitaker, J. S. Olson, R. J. Vali, A. J. Mathews, Quaternary structure regulates hemin dissociation from human hemoglobin. *J. Biol. Chem.* **272**, 17385–17389 (1997).
27. J. O. Thomas, S. J. Edelstein, Observation of the dissociation of unliganded hemoglobin. *J. Biol. Chem.* **247**, 7870–7874 (1972).
28. D. A. Gell, Structure and function of haemoglobins. *Blood Cells Mol. Dis.* **70**, 13–42 (2018).
29. R. Macdonald, B. J. Mahoney, K. Ellis-Guardiola, A. Maresso, R. T. Clubb, NMR experiments redefine the hemoglobin binding properties of bacterial NEAr-iron transporter domains. *Protein Sci.* **28**, 1513–1523 (2019).
30. P. P. Samuel *et al.*, The interplay between molten globules and heme disassociation defines human hemoglobin disassembly. *Biophys. J.* **118**, 1381–1400 (2020).
31. N. Muryoi *et al.*, Demonstration of the iron-regulated surface determinant (Isd) heme transfer pathway in Staphylococcus aureus. *J. Biol. Chem.* **283**, 28125–28136 (2008).
32. T. Spirig *et al.*, Staphylococcus aureus uses a novel multidomain receptor to break apart human hemoglobin and steal its heme. *J. Biol. Chem.* **288**, 1065–1078 (2013).
33. P. Hensley, S. J. Edelstein, D. C. Wharton, Q. H. Gibson, Conformation and spin state in methemoglobin. *J. Biol. Chem.* **250**, 952–960 (1975).
34. M. Hoshino *et al.*, Biophysical characterization of the interaction between heme and proteins responsible for heme transfer in Streptococcus pyogenes. *Biochem. Bioph. Res. Commun.* **493**, 1109–1114 (2017).
35. M. S. Hargrove *et al.*, His(64)(E7)–>Tyr apomyoglobin as a reagent for measuring rates of hemin dissociation. *J. Biol. Chem.* **269**, 4207–4214 (1994).
36. M. Sjodt *et al.*, Energetics underlying hemin extraction from human hemoglobin by Staphylococcus aureus. *J. Biol. Chem.* **293**, 6942–6957 (2018).
37. E. M. Molloy, P. D. Cotter, C. Hill, D. A. Mitchell, R. P. Ross, Streptolysin S-like virulence factors: The continuing sagA. *Nat. Rev. Microbiol.* **9**, 670–681 (2011).
38. J.M.M. Caaveiro, M. Hoshino, K. Tsumoto, Crystal structure of HID2 bound to human Hemoglobin. *Worldwide Protein Data Bank (wwPDB)* https://doi.org/10.2210/pdb7CUE/pdb deposited on 22 August 2020
39. H. Zhu, M. Liu, B. Lei, The surface protein Shr of Streptococcus pyogenes binds heme and transfers it to the streptococcal heme-binding protein Shp. *BMC Microbiol.* **8**, 15 (2008).
40. C. Lu, G. Xie, M. Liu, H. Zhu, B. Lei, Direct heme transfer reactions in the group A Streptococcus heme acquisition pathway. *PLoS One* **7**, e37556 (2012).
41. R. T. Francis Jr., J. W. Booth, R. R. Becker, Uptake of iron from hemoglobin and the haptoglobin-hemoglobin complex by hemolytic bacteria. *Int. J. Biochem.* **17**, 767–773 (1985).
42. C. B. F. Andersen *et al.*, Structure of the haptoglobin-haemoglobin complex. *Nature* **489**, 456–459 (2012).
43. M. Kristiansen *et al.*, Identification of the haemoglobin scavenger receptor. *Nature* **409**, 198–201 (2001).
44. T. L. Mollan *et al.*, Redox properties of human hemoglobin in complex with fractionated dimeric and polymeric human haptoglobin. *Free Radic. Biol. Med.* **69**, 265–277 (2014).
45. A. S. Benitez Cardenas, P. P. Samuel, J. S. Olson, Current challenges in the development of acellular hemoglobin oxygen carriers by protein engineering. *Shock* **52**, 28–40 (2019).
46. Y. Nishina, S. Miyoshi, A. Nagase, S. Shinoda, Significant role of an exocellular protease in utilization of heme by Vibrio vulnificus. *Infect. Immun.* **60**, 2128–2132 (1992).
47. B. R. Otto, S. J. M. Van Dooren, J. H. Nuijens, J. Luirink, B. Oudega, Characterization of a hemoglobin protease secreted by the pathogenic Escherichia coli strain EB1. *J. Exp. Med.* **188**, 1091–1103 (1998).
48. J. P. Lewis, J. A. Dawson, J. C. Hannis, D. Muddiman, F. L. Macrina, Hemoglobinase activity of the lysine gingipain protease (Kgp) of Porphyromonas gingivalis W83. *J. Bacteriol.* **181**, 4905–4913 (1999).
49. G. Vauquelin, S. J. Charlton, Exploring avidity: Understanding the potential gains in functional affinity and target residence time of bivalent and heterobivalent ligands. *Br J. Pharmacol.* **168**, 1771–1785 (2013).
50. S. Erlendsson, K. Teilum, Binding revisited-avidity in cellular function and signaling. *Front. Mol. Biosci.* **7**, 615565 (2020).
51. K. Krishna Kumar *et al.*, Structural basis for hemoglobin capture by Staphylococcus aureus cell-surface protein, IsdH. *J. Biol. Chem.* **286**, 38439–38447 (2011).
52. K. Krishna Kumar, D. A. Jacques, J. M. Guss, D. A. Gell, The structure of α-haemoglobin in complex with a haemoglobin-binding domain from Staphylococcus aureus reveals the elusive α-haemoglobin dimerization interface. *Acta Crystallogr. F Struct. Biol. Commun.* **70**, 1032–1037 (2014).
53. C. F. Dickson *et al.*, Structure of the hemoglobin-IsdH complex reveals the molecular basis of iron capture by Staphylococcus aureus. *J. Biol. Chem.* **289**, 6728–6738 (2014).
54. C. F. Dickson, D. A. Jacques, R. T. Clubb, J. M. Guss, D. A. Gell, The structure of haemoglobin bound to the haemoglobin receptor IsdH from Staphylococcus aureus shows disruption of the native α-globin haem pocket. *Acta Crystallogr. D Biol. Crystallogr.* **71**, 1295–1306 (2015).
55. C. F. M. Bowden *et al.*, Structure–function analyses reveal key features in Staphylococcus aureus IsdB-associated unfolding of the heme-binding pocket of human hemoglobin. *J. Biol. Chem.* **293**, 177–190 (2018).
56. O. De Bei *et al.*, Cryo-EM structures of staphylococcal IsdB bound to human hemoglobin reveal the process of heme extraction. *Proc. Natl. Acad. Sci. U.S.A.* **119**, e2116708119 (2022).
57. L. A. Lewis, E. Gray, Y. P. Wang, B. A. Roe, D. W. Dyer, Molecular characterization of hpuAB, the haemoglobin–haptoglobin-utilization operon of Neisseria meningitidis. *Mol. Microbiol.* **23**, 737–749 (1997).
58. C. T. Wong *et al.*, Structural analysis of haemoglobin binding by HpuA from the Neisseriaceae family. *Nat. Commun.* **6**, 10172 (2015).
59. K. Stødkilde, M. Torvund-Jensen, S. K. Moestrup, C. B. F. Andersen, Structural basis for trypanosomal haem acquisition and susceptibility to the host innate immune system. *Nat. Commun.* **5**, 5487 (2014).
60. H. Lane-Serff, P. Macgregor, E. D. Lowe, M. Carrington, M. K. Higgins, Structural basis for ligand and innate immunity factor uptake by the trypanosome haptoglobin-haemoglobin receptor. *Elife* **3**, e05553 (2014).
61. H. Lane-Serff *et al.*, Evolutionary diversification of the trypanosome haptoglobin-haemoglobin receptor from an ancestral haemoglobin receptor. *Elife* **5**, e13044 (2016).
62. K. H. Rohde, D. W. Dyer, Analysis of haptoglobin and hemoglobin-haptoglobin interactions with the Neisseria meningitidis TonB-dependent receptor HpuAB by flow cytometry. *Infect. Immun.* **72**, 2494–2506 (2004).
63. K. Ellis-Guardiola *et al.*, The Staphylococcus aureus IsdH receptor forms a dynamic complex with human hemoglobin that triggers heme release via two distinct hot spots. *J. Mol. Biol.* **432**, 1064–1082 (2020).
64. J. Clayton *et al.*, Directed Inter-domain motions enable the IsdH Staphylococcus aureus receptor to rapidly extract heme from human hemoglobin. *J. Mol. Biol.* **434**, 167623 (2022).
65. S. Valenciano-Bellido *et al.*, Structure and role of the linker domain of the iron surface-determinant protein IsdH in heme transportation in Staphylococcus aureus. *J. Biol. Chem.* **298**, 101995 (2022).
66. W. Kabsch, Integration, scaling, space-group assignment and post-refinement. *Acta Crystallogr. D Biol. Crystallogr.* **66**, 133–144 (2010).
67. A. J. McCoy *et al.*, Phaser crystallographic software. *J. Appl. Crystallogr.* **40**, 658–674 (2007).
68. P. Emsley, B. Lohkamp, W. G. Scott, K. Cowtan, Features and development of Coot. *Acta Crystallogr. D Biol. Crystallogr.* **66**, 486–501 (2010).
69. G. Bricogne *et al.*, BUSTER (Version 2.10.4, Global Phasing Ltd., Cambridge, UK, 2021).

70. F. W. J. Teale, Cleavage of the haem-protein link by acid methylethylketone. *Biochim. Biophys. Acta* **35**, 543 (1959).
71. T. Asakura, S. Minakami, Y. Yoneyama, H. Yoshikawa, Combination of globin and it's derivatives with hemins and porphyrins*. *J. Biochem.* **56**, 594–600 (1964).
72. K. Ellis-Guardiola, J. Soule, R. T. Clubb, Methods for the extraction of heme prosthetic groups from hemoproteins. *Bio. Protoc.* **11**, e4156 (2021).
73. F. Delaglio *et al.*, NMRPipe: A multidimensional spectral processing system based on UNIX pipes. *J. Biomol. NMR* **6**, 277–293 (1995).
74. W. Lee, M. Tonelli, J. L. Markley, NMRFAM-SPARKY: Enhanced software for biomolecular NMR spectroscopy. *Bioinformatics* **31**, 1325–1327 (2015).
75. M. T. Marty *et al.*, Bayesian deconvolution of mass and ion mobility spectra: From binary interactions to polydisperse ensembles. *Anal. Chem.* **87**, 4370–4376 (2015).
76. S. Classen *et al.*, Implementation and performance of SIBYLS: A dual endstation small-angle X-ray scattering and macromolecular crystallography beamline at the Advanced Light Source. *J. Appl. Crystallogr.* **46**, 1–13 (2013).
77. K. Manalastas-Cantos *et al.*, ATSAS 3.0: Expanded functionality and new tools for small-angle scattering data analysis. *J. Appl. Crystallogr.* **54**, 343–355 (2021).
78. J. B. Hopkins, R. E. Gillilan, S. Skou, BioXTAS RAW: Improvements to a free open-source program for small-angle X-ray scattering data reduction and analysis. *J. Appl. Crystallogr.* **50**, 1545–1553 (2017).
79. M. Pelikan, G. Hura, M. Hammel, Structure and flexibility within proteins as identified through small angle X-ray scattering. *Gen. Physiol. Biophys.* **28**, 174–189 (2009).
80. M. Ramsay, J. M. Brendan, C. Duilio, T. C. Robert, Crystal structure of the Shr Hemoglobin Interacting Domain 2 (HID2) in complex with Hemoglobin. *Worldwide Protein Data Bank (wwPDB)* https://doi.org/10.2210/pdb8DOV/pdb. deposited Jul 17, 2022.